第 36 卷第 3 期
2020 年 3 月

无 机 化 学 学 报
CHINESE JOURNAL OF INORGANIC CHEMISTRY

Vol.36 No.3
555-565

氯离子伏安刻蚀制备高活性多孔银膜及其对三氯乙酸的电化学检测

褚有群　王玲巧　黄章烤　徐颖华　赵峰鸣*

(浙江工业大学化学工程学院,绿色化学合成技术国家重点实验室培育基地,杭州　310032)

摘要：采用无机阴离子促进的伏安刻蚀技术在银线表面制备高活性多孔银膜。优选的氯离子在伏安条件下通过微反应刻蚀,促使银丝表面形成自支撑的多孔通道。当在银丝电极上施加连续的正电位后,银电极表面在氯离子作用下快速形成 AgCl 膜,经施加的电位反向,在电化学还原作用下氯离子剥离,AgCl 膜自发转化为自支撑的多孔银膜。研究表明,制备的多孔银膜(p-Ag film)对三氯乙酸具有较高的电催化活性,与原始银丝(r-Ag wire)相比,电化学活性表面积和电催化性能分别提高了 174 和 3.7 倍。将其用于三氯乙酸的电化学检测时,在浓度为 0.1~518.1 μmol·L^{-1} 范围内,制备的多孔银膜电极的最低检测限可达 70 nmol·L^{-1}(拟合相关性系数 R^2=0.998 3)。

关键词：银；阴离子；氯离子；多孔结构；电化学；传感器

中图分类号：O646.5　　**文献标识码**：A　　**文章编号**：1001-4861(2020)03-0555-11

DOI：10.11862/CJIC.2020.059

Highly Activated Polyporous Silver Film: Preparation by Voltammetric Etching with Chloride Ion Promotion and Electrochemical Determination of Trichloroacetic Acid

CHU You-Qun　WANG Ling-Qiao　HUANG Zhang-Kao　XU Ying-Hua　ZHAO Feng-Ming*

(*State Key Laboratory Breeding Base of Green Chemistry-Synthesis Technology, College of Chemical Engineering, Zhejiang University of Technology, Hangzhou* 310032, *China*)

Abstract: A highly activated polyporous silver film was constructed on the outer ring of silver wire by voltammetric etching using halogen anions. In particular, chloride ion etching can promote the formation of self-supported porous channel structure on silver wire surface via microcell reactions. Appling a continuous positive potential to the silver wire electrode contributes to form a thin film of AgCl. After electrochemical reduction, chloride ions are stripped from AgCl and the AgCl spontaneously transformed to self-supported polyporous silver film. The as prepared self-supported polyporous silver film electrode (p-Ag film) reveals substantial electrocatalytic activity for the selective and sensitive sensing of trichloroacetic acid. The p-Ag film electrode displays 174 and 3.7 times enhancement in electrochemical active surface area and the dechlorination reaction, relative to the pristine silver wire electrode (r-Ag wire). The novel electrodes exhibited a low detection limit of 70 nmol·L^{-1} (fitting correlation coefficient R^2=0.998 3) with the trichloroacetic acid concentration range of 0.1~518.1 μmol·L^{-1}.

Keywords: silver; anions; chlorine; polyporous structure; electrochemistry; sensors

收稿日期:2019-10-10。收修改稿日期:2019-12-06。

浙江省自然科学基金(No.LY17B050006)和国家重点研究开发计划(No.2017YFB0307503)资助项目。

*通信联系人。E-mail:zhaofm@zjut.edu.cn

0 Introduction

Trichloroacetic acid (TCA), a non-biodegradable organohalide pollutant, can be found in drinking water, swimming pool, agricultural and industrial waste water since the addition of chlorine to water for chlorination disinfection[1-4]. It has been urgently appealed to make site monitoring over the concentration of TCA due to its carcinogenic and mutagenic effects[5-6]. Electroanalytical techniques coupled with modified electrodes have the merits of rapid detection, low consumption and on-site monitoring, which cannot be obtained by other methods, such as chromatographic[7], microextraction[8], electrophoresis[9]. A great deal of efforts have been put into developing non-enzymatic electrochemical sensors based on metal nano-modified electrodes owing to its electrocatalytic ability, stability and reliability, such as Pd/Fe[10], AgPd[11], Cu[12], Au@Ag[13], Ag[14]. Among the developed metal nano-modified electrodes for the determination of TCA, Liu et al.[15] reported the electrode by controlled electrodeposition of silver nanoparticles on chitosan hydrogel film to detect TCA with acceptable selectivity. Bashami et al.[16] fabricated a highly conductive thin film composite using the casting solution of malic acid functionalized silver nanoparticles as a precursor. Chen et al.[17] proposed the free-standing nanoporous silver by selective dissolution of $Au_{42}Ag_{58}$ alloys while inert component (Au) is dissolved. Although the above studies have achieved good results, we noticed that all the prepared electrocatalysts are coated on a glassy carbon electrode by physical combination in experimental methods. This is extremely worrying for their binding force, fastness and repetitive. Once detached, the test results were inaccurate. To our great pity, until now, wires, rods, plates or other metal electrode did not be directly used for TCA detection due to their low electrocatalytic activity for electrochemical reduction. It is an attention-worth problem that a surface activated layer should be formed on the metal materials by the surface activation technique so that it can be directly used as TCA- sensing electrode.

Recently, self-supported nanoporous metal electrodes are becoming more and more attractive due to the rich porous structure, high surface area and excellent electrocatalytic performance[18-21]. For instance, Yuan et al.[22] prepared a series of freestanding 3D nanoporous silver from silver metal sheet by electrochemical approach. The prepared electrode displayed 130 and 11.5 times enhancement in catalytic activity for oxygen reduction and formaldehyde electrooxidation, relative to the flat silver electrode. Li et al.[23] aimed at exploring an approach to prepare the self-supported nanoporous silver electrode, which showed good catalytic activity for oxygen reduction and electrochemically stability with methanol tolerance property, compared to the pristine silver electrode. In previous works of our team, many silver electrodes, such as roughened silver-palladium[24], silver disk[25], silver meshes[26], silver plates[27-28], and silver nanoparticles[29], were applied for electrochemical reduction of halogenated organic compounds, showing excellent electrocatalytic performance. In this work, we focus on a voltammetric etching approach to spontaneously produce the activated polyporous silver film on the surface of silver wire. The influences of different anions, such as HCO_3^-, CO_3^{2-}, SO_4^{2-} and Cl^-, were investigated and chloride ions was considered as an important factor to promote the spontaneous formation of self-supported polyporous film on silver surface through a micro-chemical reaction. A sensitive amperometric sensor with highly activated polyporous silver film electrode displayed low limit detection for TCA.

1 Experimental

1.1 Materials

Sliver wire (ϕ=0.5 mm) was derived from Tianjin Incole Union Technology Co., Ltd. Trichloroacetic acid (TCA) was 99% purity and purchased from Aladdin Reagent Co., China. Sulfuric acid (H_2SO_4, 98%(*w*/*w*)), nitric acid (HNO_3, 98% (*w*/*w*)) were obtained from Xilong Scientific Co., Ltd, and sodium chloride(NaCl, 99.5%(*w*/*w*)) were bought from Shanghai No.4 Reagent & H.V. Chemical Co., Ltd. Phosphate buffer solutions (PBS) with pH =7.0 were prepared by mixing the monopotassium phosphate (KH_2PO_4, 0.02 mol·L^{-1}) and

potassium hydroxide (KOH, 0.02 mol·L^{-1}).

1.2 Instrumentation

The morphology of silver electrode was examined by high angle annular dark field scanning electron microscopy (SEM) coupled with energy dispersive X-ray spectrometer (EDX), using Cu $K\alpha$ radiation at an acceleration voltage of 15.0 kV. X-ray diffraction (XRD) patterns were obtained using Netherlands PNAlytical X′Pert PRO X-ray diffractometer equipped with Cu $K\alpha$ radiation (λ=0.154 1 nm, 40 kV, 40 mA). Samples were scanned from 10° to 110° at a step of 0.033°. The oxidation states of chemical species were detected by X-ray photoelectron spectroscopy (XPS, Kratos Axis Ultra DLD) using a focused monochromatized Al $K\alpha$ operated at 300 W. The binding energies were referenced to the C1*s* line at 284.6 eV from adventitious carbon.

1.3 Preparation of activated self-supported polyporous silver film

Silver wire was sonicated in acetone, and then polished to a mirror finish using 1.0 mol·L^{-1} nitric acid. The polished silver wire was washed with ethanol and deionized water water. The silver wire after pretreatment was saved in the deoxygenated anhydrous ethanol. Firstly, the silver wire (L=5.0 cm) was fixed 1.0 cm for etching, and the excess parts were covered up. Then, the prepared silver wire was synthesized in a 10 mL three-electrode cell, as the working electrode, platinum wire (L=0.5 mm) as the counter electrode and Ag/AgCl electrode as the reference electrode. The voltammetric etching was controlled by electrochemical workstation (Ivium potentiostat). The silver wire was carried out by voltammetric scans in a range of −1.0 to 1.0 V, scanning rate of 50 mV·s^{-1}. After two cycles, the self-supported polyporous silver film electrode (p-Ag film) was prepared.

1.4 Calculation of electrode roughness factor

The roughness factor is the actual electrochemical surface area of the electrode measured relative to pure metallic mercury per square centimeter. The roughness factor (ρ) of silver electrodes was measured by small amplitude potential step method. The definition of roughness factor is as follows[30-31]:

$$\rho=\frac{\int_0^t (i-i_\infty)\mathrm{d}t}{\Delta\varphi C_N A_P}$$

where i is the apparent current (mA); i_∞ is the steady current after step (mA); t is the second phase of the current acquisition time (10 s); $\Delta\varphi$ is the step amplitude (100 mV); A_P is the apparent area of the electrode (1.57 cm^2); C_N is the double layer capacitor of pure mercury (20 μF·cm^{-2}). The roughness of the silver wire electrocdes were exposed through the electrochemical detection methods of constant potential step in 1.0 mol·L^{-1} TCA aqueous solution.

1.5 Electrochemical measurement

Electrochemical performance measurements of trichloroacetic acid (TCA) was revealed in a potential range of 0 to −1.2 V at a scan rate of 20 mV·s^{-1}, using a three-electrode cell with the p-Ag film as working electrodes, a platinum foil counter electrode, and an Ag/AgCl reference electrode. The chronoamperometry was performed on a CHI600D potentiostat at −0.6 V. The detection performance analysis was conducted by different concentrations of TCA solutions added to the N_2-satruated 0.02 mol·L^{-1} PBS (6 mL, pH =7.0). The sensitivivity, stability, reproducibility and anti-interfering activity of p-Ag film for electrochemical sensing TCA were also performed at −0.6 V.

2 Results and discussion

2.1 Influence of anions on the spontaneous formation of polyporous silver film

A simple and fast method of voltammetric etching was adopted to form a highly activated self-supporting film on the surface of silver wire electrode. The anions were inserted into the silver crystal lattice to control the crystals to generate self-supported polyporous silver film. Fig.1 shows the schematic of voltammetric etching in different anions (R^-).

The pristine silver wire electrode (r-Ag wire) was oxidized firstly to form the intermediate oxidation silver state (o-Ag state) in the synergy of different anions by voltammetric oxidation from 0 to 1.0 V. Then, the voltammetric reduction was carried out to fabricate the self-supported polyporous silver film

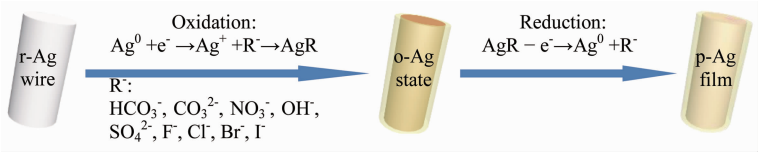

Fig.1 Schematic of voltammetric etching in different anions (R^-), anions including HCO_3^-, CO_3^{2-}, NO_3^-, OH^-, SO_4^{2-}, F^-, Cl^-, Br^-, I^-

electrode (p-Ag film) from 0 to −1.0 V. The anions included HCO_3^-, CO_3^{2-}, NO_3^-, OH^-, SO_4^{2-}, F^-, Cl^-, Br^-, I^-. The activation of the silver wire electrode by voltammetric etching using different anions is provided in Fig.S1 and Fig.S2 in the supporting information.

The activation degree of different anions on the surface of silver wire was analyzed by constant potential step method in Fig.2. The ρ of the silver electrodes after voltammetric etching was showed in Table 1 (data from the Fig.2). The roughness factor of the silver wire etched by chloride ion was 14.475 5 $cm^2\cdot cm^{-2}$. The values of other activated electrodes were all less than 6 $cm^2\cdot cm^{-2}$. The results show the better anion electrolytic etchant was chloridion. The electrochemical performance of silver wire etched by different anions was shown in Fig.S3. The silver wire electrode etched by chloride ion has significant current response towards 1.0 mmol·L^{-1} TCA. The major detected compounds were chlorinated organics, so the Cl^- activtion electrodes can be more beneficial. Fig.S4 shows the constant potential step about the surface roughness of the r-Ag wire. The ρ of the r-Ag wire was calculated about 0.083 2 $cm^2\cdot cm^{-2}$ from Fig. S4. The p-Ag film by voltammetric etching containing

Table 1 Value of ρ calculated from Fig.2

Anion	Integral area	ρ / ($cm^2\cdot cm^{-2}$)
HCO_3^-	17.946 5	5.715 4
CO_3^{2-}	18.412 2	5.863 8
NO_3^-	9.442 4	3.007 1
OH^-	4.310 1	1.372 6
SO_4^{2-}	2.873 6	0.915 1
F^-	14.869 9	4.735 6
Cl^-	45.453 1	14.475 5
Br^-	18.092 9	5.762 1
I^-	3.939 0	1.254 5
r-Ag wire	0.261 3	0.083 2

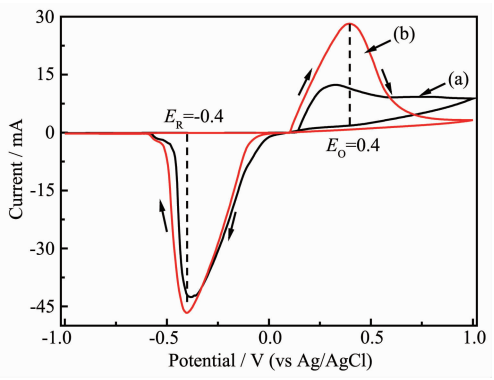

(a) First cycle; (b) Second cycle

Fig.3 Activation of the silver wire electrodes by voltammetric etching in 0.5 mol·L^{-1} NaCl with scan rate of 50 mV·s^{-1}

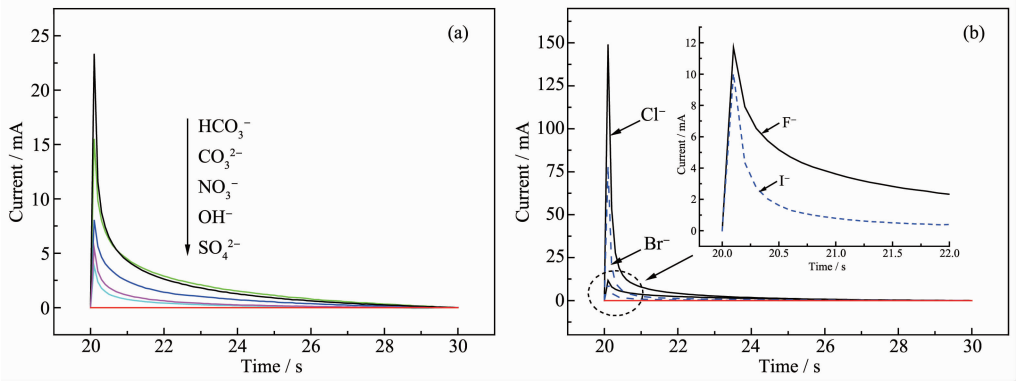

(a) Including NO_3^-, SO_4^{2-}, CO_3^{2-}, HCO_3^-, OH^-; (b) Including F^-, Cl^-, Br^-, I^-

Fig.2 Constant potential step of silver electrodes after voltammetric etching in different anions

chloride anion had the largest roughness, which was about 174 times higher than that of the r-Ag wire.

Fig.3 shows the activation of the silver wire electrode by voltammetric etching. The activate fluid was a solution of 0.5 mol·L^{-1} NaCl and the activated process was two cycles voltammetric etching from −1.0 to 1.0 V (Fig.S5 and Fig.S6). The oxidation peak (E_O) at 0.4 V was attributed to the oxidation of Ag+e$^-$ → Ag$^+$, and then the chloridion was inserted into the silver crystal lattice to obtain the AgCl crystals. The reduction peak (E_R) at −0.4 V was attributed to the reduction of AgCl-e$^-$ → Ag+Cl$^-$. The cyclic voltammograms curves (CVs) of the first and second voltammetric etching were compared in Fig.3(a,b). It is obvious that the oxidation capacity of the second cycle was stronger than the first one. It is mainly caused by the smooth surface of silver wire after pre-cleaned, leding to the oxidation of silver element only existed in superficial silver wire. The intermediate oxidation state of AgCl soild covered the electrode, compelling chloride ion difficult to infiltrate into the internal of silver wire. After the first cycle, there are a large number of holes in the surface of silver wire due to abscission of chloridion. It is easier than the first cycle for chloridion to insert into the silver crystal lattice as result of the chloride ions permeate into the silver wire electrode, meanwhile it makes the more silver element oxidized to Ag$^+$ ion. It is better to select two cycles voltammetry for electrochemical etching.

2.2 Characterization of polyporous silver film

Fig.4 shows the SEM images of the surface structure about silver wire electrode before and after voltammetric etching. Before etching (Fig.4a), the surface of the pristine silver wire (r-Ag wire) was smooth and the intermediate oxidation state (o-Ag state) sticks to skin layer, generating the nanospheres to pile up, and enhancing the roughness (Fig.4c). With the reduction reaction of Ag$^+$ and the departure of Cl$^-$, Fig.4b presents the porous structure to form the self-supported polyporous film (p-Ag film). Fig.4e shows the secondary pores of p-Ag film gather in size from 0.2 to 0.6 μm. Fig.4d shows the cross section for p-Ag film of the thickness was 8~9 μm.

Fig.5 shows the XRD patterns of pristine silver wire (r-Ag wire), intermediate oxidation state (o-Ag state) and polyporous silver film (p-Ag film). For the r-Ag wire, the diffraction peaks at 2θ=38.2°, 44.3°, 64.5°, 77.4° and 81.6° can be indexed to the (111), (200), (220), (311) and (222) crystal planes of metallic Ag[32], respectively. When the r-Ag wire was etched in the synergy of chloride anion, the o-Ag state exhibited the distinct diffraction peaks at approximately 2θ = 27.8°, 32.2° and 44.3°, which were attributed to the (111), (200) and (220) crystal planes of AgCl [33], respectively. When the o-Ag state was electrochemical reducted, the p-Ag film had the same XRD patterns as that of the r-Ag wire. It indicates that the intermediate state of silver wire formed Ag/AgCl crystals. Further,

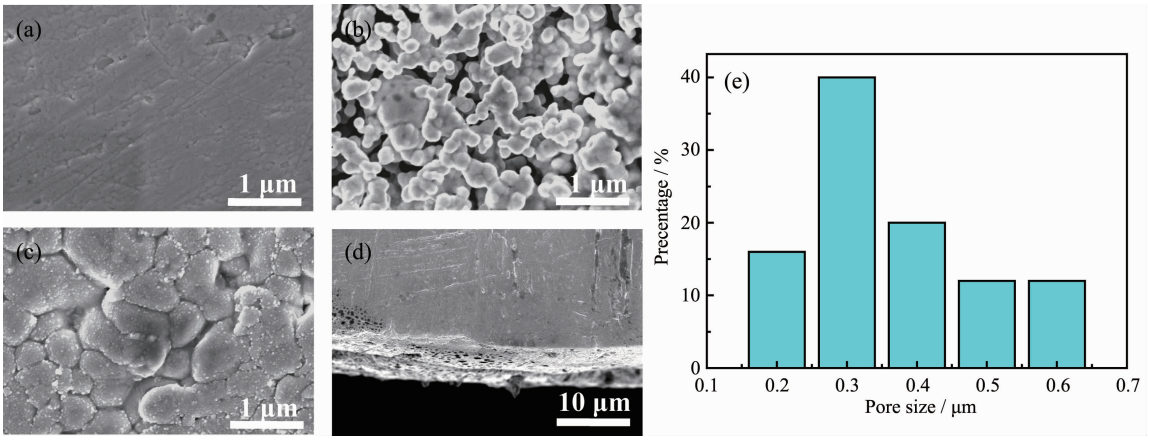

Fig.4　SEM images of (a) r-Ag wire, (b) p-Ag film, (c) o-Ag state and (d) cross section of p-Ag film; (e) Size histograms of the secondary pores of p-Ag film

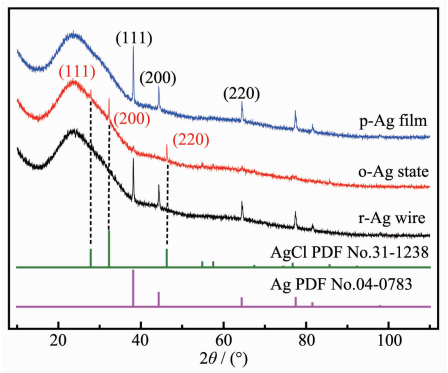

Fig.5 XRD patterns of silver wire electrodes

the present of both Ag and Cl in the etching process was confirmed by energy dispersive X-ray spectroscopy (EDS) (Fig.S7), suggesting that the oxidited Ag was present in its solid AgCl form. The EDS elemental mapping of Ag and Cl was homogeneously distributed throughout the Ag network[34], wherein the semi-quantitative analysis (Table S1) shows that the molar radio between Ag and Cl was about 3.4. The data is beneficial attest that the oxidation state of sliver element was AgCl.

To further confirm the surface elemental composition and chemical state of the prepared p-Ag film, XPS was carried out (Fig.6). The survey XPS spectrum reveals that the surface of p-Ag film was composed of Ag, Cl and O element, which agrees with EDS and XRD measurement. Table S2 shows the atom ratio about the electrochemical etching of Cl to Ag was approximately 1:1. The high-resolution XPS spectra of Ag3*d* of r-Ag wire and p-Ag film in Fig.6b shows that the characteristic peak of Ag3$d_{5/2}$ and Ag3$d_{3/2}$ were centered at 368.2 and 374.2 eV, respectively. According to the literature[35,38], the peak of the r-Ag wire and p-Ag film at 368.2 and 374.2 eV can be attributed to the Ag species. The peak of o-Ag state in Fig.6b2 shows the characteristic peak of Ag3$d_{5/2}$ and Ag3$d_{3/2}$ at 367.1 and 373.1 eV, respectively. The peak of the o-Ag state at 367.1 and 373.1 eV can be assigned to the Ag^+ species of AgCl. From the literatures[39,41], the two peaks at the binding energies of 199.1 and 197.5 eV can be ascribed to Cl2$p_{1/2}$ and Cl2$p_{3/2}$ in Fig.6c2. It provides the favorable evidence that the o-Ag state is AgCl crystale during the electrochemical etching process.

The activation mechanism of silver wire electrodes is reflected in Fig.7. The r-Ag wire was immersed in 0.5 mol·L^{-1} NaCl solution. It is Ag element around the face of r-Ag wire transformed into Ag^+ ion. Because a lot of the chloridion are permeaed into the silver crystal lattice, Ag^+ and Cl^- are combined rapidly into AgCl crystals on the surface layer of silver wire electrodes. There is a stratum AgCl oxidation film to wrap the silver wire electrodes. The response equation is:

$$Ag\text{-}e^-+Cl^- \longrightarrow AgCl \quad (1)$$

Then, also in the 0.5 mol·L^{-1} NaCl solution, the AgCl crystals are destroyed for the absence of Cl^- ion.

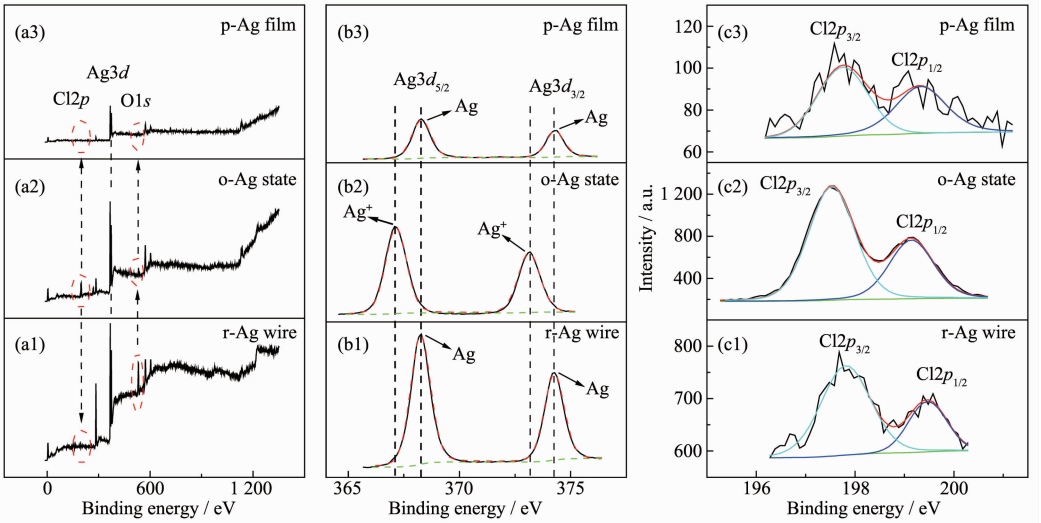

Fig.6 (a) XPS spectra of silver wire; High-resolution XPS spectra of (b) Ag3*d* and (c) Cl2*p* of silver wire

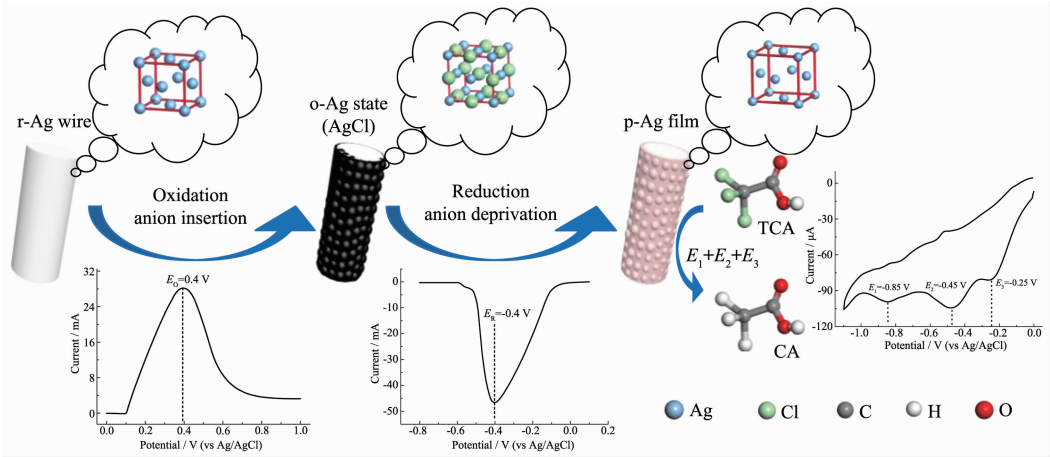

Fig.7　Schematic showing the steps involved in the ion transfer of the voltammetric etching silver wire electrode

The Ag^+ ion is restored into Ag element, adhered to the surface of electrode. The reduced equation is:

$$AgCl+e^- \longrightarrow Ag+Cl^- \quad (2)$$

The Ag elements attach to the surface of the activated silver wire electrode after voltammetric etching shows porous structure. The roughness of p-Ag film is larger than the r-Ag wire.

2.3　Electrochemical behavior of the p-Ag film

The electrochemical behaviors of r-Ag wire and p-Ag film were examined by cyclic voltammograms in 1.0 mmol·L^{-1} TCA and 60 mL PBS with pH=7.0. Fig. 8a shows the CVs of r-Ag wire and p-Ag film in the PBS. The electrochemical performance of r-Ag wire electrode in PBS displays only one observable peak. The p-Ag film electrode obviously exhibited three distinct reduction peaks for detecting TCA. The results indicate that activated elemental silver on the electrodes surface can easily capture the TCA molecule in solution. Fig.8b shows the CVs of p-Ag film with 1.0 mmol·L^{-1} trichloroacetic acid (TCA), dichloroacetic acid (DCA), or monochloroacetic acid (MCA). The peak of MCA showed one reduction potential at about −0.85 V, the peaks of DCA showed two reduction potential at about −0.85 and −0.45 V, and the peaks of TCA showed three reduction potential at about −0.85, −0.45, and −0.25 V.

The reduction of TCA involves three Cl atoms in the TCA molecule dechlorination reaction route, which can be confirmed from three reduction peaks in the Fig.8b. The first reduction peak nearby −0.25 V indicates the first Cl atom in the TCA in the reaction equation[16]:

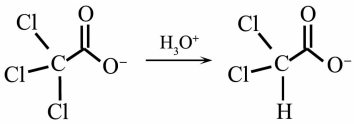

(3)

The second reduction peak around −0.45 V demonstrates the second Cl atom in the TCA in the reaction equation:

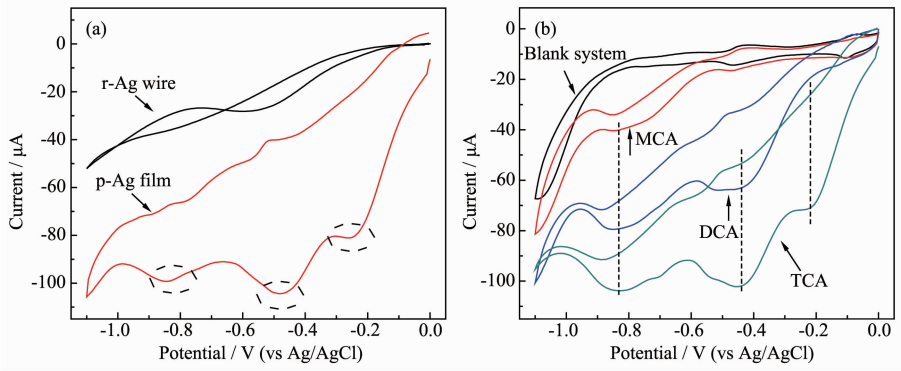

Fig.8　(a) CVs of r-Ag wire and p-Ag film in 1.0 mmol·L^{-1} TCA and pH=7 PBS at 20 mV·s^{-1}; (b) CVs of p-Ag film in 1.0 mmol·L^{-1} MCA, DCA and TCA at 20 mV·s^{-1}

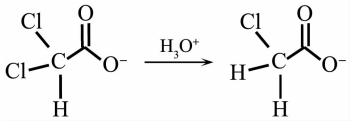

(4)

The third reduction peak beside −0.85 V represents the third Cl atom in the TCA in the reaction equation:

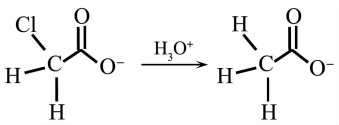

(5)

Fig.9 shows the cyclic voltammetry of TCA in the concentration range from 0.2 to 5.0 mmol·L^{-1}. With the increasing of TCA concentration, the reduction peak currents increased from −100 to −500 μA, nevertheless the reduction peak potential at −0.85 V deviated to −0.95 V. It indicates that the carboxylic group of TCA may interact with the silver element, which leads to a negative shift in potential.

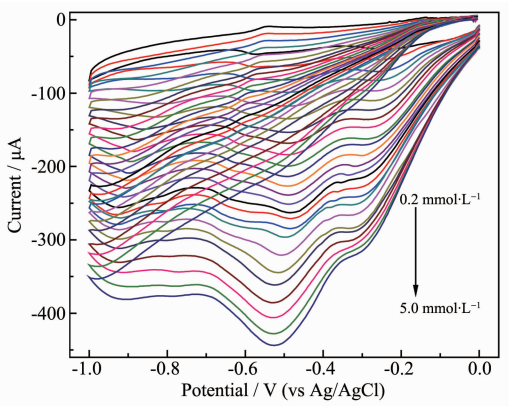

C_{TCA}=0.2, 0.4, 0.6, 0.8, 1.0, 1.2, 1.4, 1.6, 1.8, 2.0, 2.2, 2.4, 2.6, 2.8, 3.0, 3.2, 3.4, 3.6, 3.8, 4.0, 4.2, 4.4, 4.6, 4.8, 5.0 mmol·L^{-1}; Scan rate: 20 mV·s^{-1}

Fig.9 CVs of p-Ag film in the successive addition of different concentrations of TCA

2.4 Amperometric detection of trichloroacetic acid

Fig.S9 exhibits the amperometric responses of p-Ag film at different potentials. The amperometry responses of 10 μmol·L^{-1} TCA at −0.6 V were greater than the other potentials from −0.1 to −0.5 V. The amperometric *i-t* curves were performed with the successive addition of TCA into a stirring electrochemical cell containing 6 mL PBS (0.02 mol·L^{-1}, pH=7.0) at an optimized potential of −0.6 V (Fig.10a). The current response of TCA attained a stable state within 3 s as a result of the excellent electrocatalytic activity of polyporous structure. Fig.10b presents the linear fitting relationships between the current responses. The linear regression equations of p-Ag film was i=0.182 6C_{TCA}+2.820 8 (fitting correlation coefficient R^2=0.998 3), where i (0.1~518.1 μmol·L^{-1}) is the current and C_{TCA} is the concentration of TCA. The limit of detection (LOD) is determined using the equation LOD=3S_B/b, where b is the slope of the calibration curve and S_B is the standard deviation of the blank solution. The LOD (S/N=3) of p-Ag film sensor was calculated to be 70 nmol·L^{-1}. Table 2 shows the modified electrodes in the references. The results demonstrate that p-Ag film provides a facile but effective electrochemical sensor to detect TCA.

Fig.11 shows the effects of interferents such as glucose, citric acid, ascorbic acid, acetic acid, and NaCl at −0.6 V on TCA. It can be seen, adding

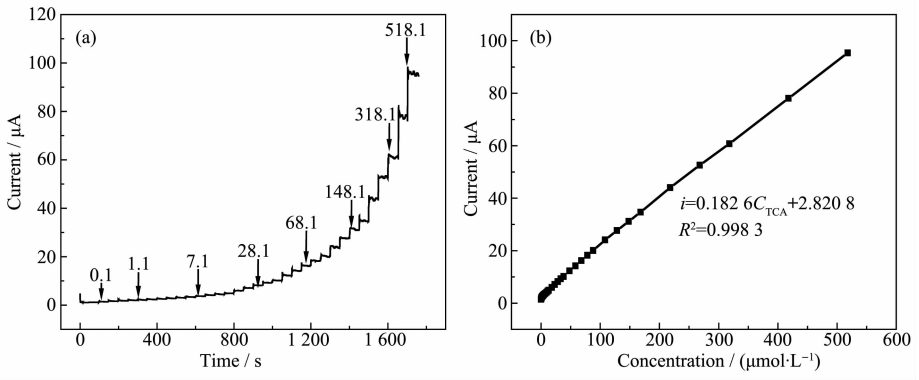

Fig.10 (a) Amperometry responses of p-Ag film sensor at −0.6 V with successive addition of TCA in PBS (pH=7.0, C_{TCA} was from 0.1 to 518.1 μmol·L^{-1}); (b) Plot of i vs C_{TCA}

Table 2　Comparison of different electrodes for TCA determination

Modified electrode	Linear range / ($\mu mol \cdot L^{-1}$)	LOD / ($\mu mol \cdot L^{-1}$)	Reproducibility	Stability / %	Long-term stability	Reference
Ionic liquid-functionalized graphene-AgPd alloy nanoparticle composite	0.5~50	0.2	8.1%, 7 cycles	7.2	89.6%, 21 days	[11]
Hemoglobin on the core-shell Au@Ag nanorod	0.16~1.7	0.12	—	4.2	95%, 7 days	[13]
Silver nanoparticle coated multi-walled carbon nanotubes	5.0~120	1.9	—	<7	93%, 15 days	[14]
A highly conductive thin film composite based on silver nanoparticles and malic acid	0.1~2.0 4.0~100	0.03 0.079	3.90%	<5	95%, 30 days	[16]
Free-standing nanoporous silver	2 500~25 000	25.4	—	—	—	[17]
Hemoglobin was immobilized on the surface of carbon ionic liquid electrode with chitosan and MnO_2 nanoparticle composite materials	500~16 000	167	2.8%±0.03%, 6 cycles	—	96.8%, 14 days	[42]
Titanate nanotubes were self-assembled on the chitosan and the model electrochemical probe is thionine	0.015~1 500	—	6.31%, 6 cycles	3.78 3.04	89.3%, 14 days	[43]
p-Ag film	0.1~400	0.072	1.4%, 5 cycles	2.22	74.4%, 14 days	This work

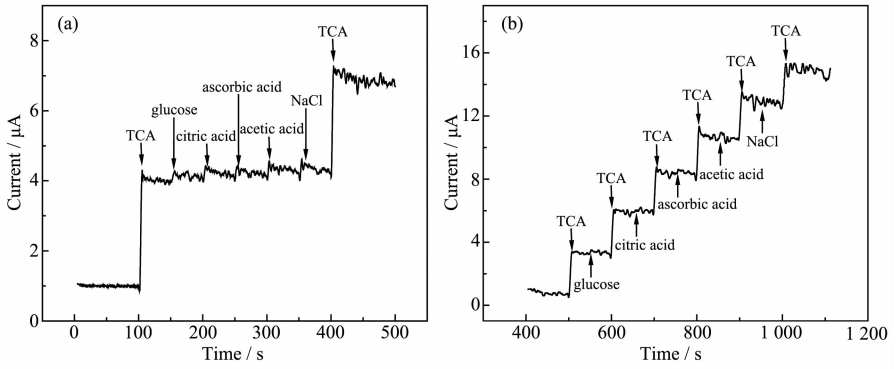

Fig.11　Amperometry responses of the p-Ag film with different interferents at −0.6 V

interferents did not show any signification response. The results indicate that the p-Ag film have an excellent selectivity for detection of TCA. The reproducibility of the p-Ag film was researched by chronoamperometry at −0.6 V with adding 0.5 and 10.0 $\mu mol \cdot L^{-1}$ TCA for 5 times (Fig.S10). The relative standard deviation (RSD) was 4.5% and 9.5%, declaring the good reproducibility. Furthermore, the p-Ag film sensor has also good stability with detection performance (Fig.S11). The properties of same electrode maintained above 90% after five tests. Furthermore, the analysis data of two identical polyporous electrodes at different times for detecting TCA were summarized. The data show that the p-Ag film electrode could maintain 89.4% and 91.2% after two weeks (Fig.S12). It implies that the silver wire electrode after voltammetric etching by Cl^- ion demonstrated an acceptable stability. It may be because the activated Ag element was not easy to fall off the surface of silver electrodes after the Cl^- ion voltam-

metric etching. However, it is important to realize that the p-Ag film must be kept in the absence of oxygen.

3 Conclusions

In summary, the activated self-supported polyporous silver film electrode (p-Ag film) was successfully fabricated by a simple voltametric etching and successfully applied in nonenzymatic electrochemical determination of TCA. The selection of anions was critical for voltametric etching. The p-Ag film can be obtained in electrolytic etchant containing chlorine than the other anions for detecting TCA. In comparison to the r-Ag wire, the p-Ag film had the greater roughness and displayed the more excellent electrochemical performance of TCA. The fabricated p-Ag film showed high reproducibility, repetition, sensitivity, and long-stability, making it effective as an electrode for determination of TCA. The amperometric characterization confirms that the linearity of the developed non-enzymatic electrochemical sensor for detection of TCA from 0.1~518.1 $\mu mol \cdot L^{-1}$ and the detection limit can reach 70 $nmol \cdot L^{-1}$ (S/N=3).

Acknowledgments: We acknowledge the financial support from the Natural Science Foundation of Zhejiang Province (Grant No.LY17B050006) and the National Key Research and Development Plan (Grant No.2017YFB0307503).

Supporting information is available at http://www.wjhxxb.cn

References:

[1] Suedee R, Intakong W, Dickert F L. *Anal. Chim. Acta*, **2006**, **569**(1/2):66-75

[2] Hu B, Wu C D, Zhang Z L, et al. *Ceram. Int.*, **2014**,**40**(5): 7015-7021

[3] Smith R B, Nieuwenhuijsen M J, Wright J, et al. *Environ. Res.*, **2013**,**126**:145-51

[4] Xie W Q, Gong Y X, Yu K X. *Biomed. Chromatogr.*, **2018**, **32**(10):e4288

[5] Esclapez M D, Tudela I, Díez-García M I, et al. *Appl. Catal. B*, **2015**,**166-167**:66-74

[6] Zhao B X, Li X, Li W J, et al. *Chem. Eng. J.*, **2015**,**273**:527-533

[7] Wang Y X, Zeng Q, Wang L, et al. *Environ. Res.*, **2014**,**135**: 126-132

[8] Saraji M, Jamshidi F, Mossaddegh M, et al. *Microchem. J.*, **2019**,**146**:914-921

[9] Martínez D, Borrull F, Calull M. *J. Chromatogr. A*, **1999**,**835**: 187-196

[10]Li A Z, Zhao X, Hou Y N, et al. *Appl. Catal. B*, **2012**,**111-112**:628-635

[11]Shang L, Zhao F Q, Zeng B Z. *Anal. Methods*, **2013**,**5**(21): 6058-6063

[12]Esclapez M D, Díez-García M I, Sáez V, et al. *Electrochim. Acta*, **2011**,**56**(24):8138-8146

[13]Qian D P, Li W B, Chen F T, et al. *Microchim. Acta*, **2017**, **184**(7):1977-1985

[14]Liu B Z, Hu X B, Deng Y H, et al. *Electrochem. Commun.*, **2010**,**12**(10):1395-1397

[15]Liu B Z, Deng Y H, Hu X B, et al. *Electrochim. Acta*, **2012**, **76**:410-415

[16]Bashami R M, Soomro M T, Khan A N, et al. *Anal. Chim. Acta*, **2018**,**1036**:33-48

[17]Chen T, Liu Z N, Lu W J, et al. *Electrochem. Commun.*, **2011**,13(10):1086-1089

[18]Shi L, Rong X J, Wang Y, et al. *Biosens. Bioelectron.*, **2018**, **102**:41-48

[19]Hong W T, Jian C Y, Wang G X, et al. *Appl. Catal. B*, **2019**,**251**:213-219

[20]Liu Y F, Xiong L Q, Li P X, et al. *J. Power Sources*, **2019**, **428**:20-26

[21]Tu F H, Xia Y, Huang W, et al. *Mater. Lett.*, **2017**,**206**:197-200

[22]Yuan L Z, Jiang L H, Zhang T R, et al. *Catal. Sci. Technol.*, **2016**,**6**(19):7163-7171

[23]Li X K, Liu J, Du F L, et al. *Appl. Surf. Sci.*, **2019**,**464**:21-29

[24]Ma C A, Ma H, Xu Y H, et al. *Electrochem. Commun.*, **2009**,**11**(11):2133-2136

[25]Xu Y H, Ding X F, Ma H X, et al. *Electrochim. Acta*, **2015**, **151**:284-288

[26]Xu Y H, Cai Q Q, Ma H X, et al. *Electrochim. Acta*, **2013**, **96**:90-96

[27]Xu Y H, Zhu Y H, Zhao F M, et al. *Appl. Catal. A*, **2007**, **324**:83-86

[28]Xu Y H, Zhang H, Chu C P, et al. *J. Electroanal. Chem.*, **2012**,**664**:39-45

[29]Zhao F M, Zhou M L, Wang L Q, et al. *J. Electroanal. Chem.*, **2019**,**833**:205-212

[30]Zhao F M, Yan F, Qian Y, et al. *J. Electroanal. Chem.*, **2013**,**698**:31-38

[31]ZHAO Feng-Ming(赵峰鸣), WEN Gang(闻刚), KONG Li-

Yao(孔丽瑶), et al. *Chinese J. Inorg. Chem.*(无机化学学报), **2017**,**33**(3):501-508

[32]Zhu Y P, Zhu R L, Xi Y F, et al. *Chem. Eng. J.*, **2018**,**346**:567-577

[33]Zhu H G, Chen D Y, Li N J, et al. *J. Colloid Interface Sci.*, **2018**,**531**:11-17

[34]Antink W H, Choi Y J, Seong K D, et al. *Sens. Actuators B*, **2018**,**255**:1995-2001

[35]Liu Q Q, Xu Y G, Wang J, et al. *Colloids Surf. A*, **2018**, **553**:114-124

[36]Zhang W D, Dong X A, Liang Y, et al. *Appl. Surf. Sci.*, **2018**,**455**:236-243

[37]Zhang C Y, Yu Y G, Wei H, et al. *Appl. Surf. Sci.*, **2018**, **456**:577-585

[38]Ding K, Wang W, Yu D, et al. *Appl. Surf. Sci.*, **2018**,**454**:101-111

[39]Xie J S, Wu C Y, Xu Z Z, et al. *Mater. Lett.*, **2019**,**234**:179-182

[40]Zhao B X, Wang X Q, Shang H, et al. *Chem. Eng. J.*, **2016**, **289**:319-329

[41]Esclapez M D, Tudela I, Díez-García M I, et al. *Chem. Eng. J.*, **2012**,197:231-241

[42]Zhu Z H, Qu L N, Niu Q J, et al. *Biosens. Bioelectron.*, **2011**,**26**(5):2119-2124

[43]Dai H, Xu H F, Wu X P, et al. *Talanta*, **2010**,**81**(4/5):1461-1466